

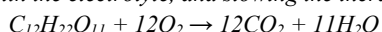
Improvement of Electrochemical Performance and Thermal Stability by Reducing Residual Lithium Hydroxide on $\text{LiNi}_{0.8}\text{Co}_{0.1}\text{Mn}_{0.1}\text{O}_2$ Active Material using Amorphous Carbon Coating

Ji-Woong Shin and Jong-Tae Son*

Department of Nano Polymer Science & Engineering, Korea National University of Transportation, Chungju, Chungbuk 380-702, Korea

Received: March 20, 2018, Accepted: April 12, 2018, Available online: April 19, 2018

Abstract: Using $\text{LiNi}_{0.8}\text{Co}_{0.1}\text{Mn}_{0.1}\text{O}_2$ as a starting material, a surface-modified cathode material was obtained by coating it with a nanolayer of amorphous carbon, where the added $\text{C}_{12}\text{H}_{22}\text{O}_{11}$ (sugar) was transformed to Li_2CO_3 compounds after reacting with residual LiOH on the surface. A thin and uniformly smooth nanolayer (35 nm thick) was observed on the surface of the $\text{LiNi}_{0.8}\text{Co}_{0.1}\text{Mn}_{0.1}\text{O}_2$, as confirmed by transmission electron microscopy (TEM). The amount of residual lithium hydroxide (LiOH) was significantly reduced through the formation of lithium carbonate (Li_2CO_3). As a result, carbon-coated $\text{LiNi}_{0.8}\text{Co}_{0.1}\text{Mn}_{0.1}\text{O}_2$ exhibited noticeable improvement in capacity and rate capability and much lower exothermic heat in the charged state at 4.3V. The improved electrochemical performance and thermal stability are attributed to the carbon coating, which reduced the residual lithium hydroxide, protected the cathode material from reacting with the electrolyte, and slowing the incrassation of the solid electrolyte interphase (SEI) film on the surfaces of the oxide particles.



PACS number: 73.20.At

Keywords: Lithium secondary battery, Cathode material, Carbon coating, $\text{C}_{12}\text{H}_{22}\text{O}_{11}$

1. INTRODUCTION

Lithium ion batteries (LIBs) have been widely and successfully employed in portable electronic devices such as mobile phones and laptop computers [1-3]. Recently, LIBs have gained recognition as one of the most promising energy storage systems for electric vehicles (EVs) and hybrid electric vehicles (HEV). However, batteries for EVs and HEVs require higher energy, long cycle life, and higher safety than conventional batteries, and they must be affordable [4-6]. Among the various cathode materials used in LIBs, Ni-rich cathode materials have attracted an increasing amount of interest due to their high capacity, relatively low cost, and low toxicity when compared to LiCoO_2 [7-8]. However, these materials have thermal and structural instabilities caused by oxygen loss from their host structures at highly delitiated states. Even worse, Ni-rich compounds always contain a large amount of residual lithium compounds such as LiOH and Li_2CO_3 [8]. The presence of lithium residues is undesirable because the oxidation of

these compounds results in the formation of Li_2O and CO_2 gas at higher voltages, which lowers the coulombic efficiency between the charge and discharge capacities during cycling [9].

Application of coating materials such as oxides [10-11], phosphates [12-13], and carbon [14-15] to the surfaces of lithium transition metal oxide particles can mitigate the problems mentioned above. These surface films reduce the dissolution of the active material by scavenging HF, thereby diminishing the increases in impedance at the interfaces, such as R_{film} and R_{ct} .

Many research works have confirmed that carbon coating can enhance electron conductivity to improve the battery's discharge capacity and rate performance [16-17]. However, the mechanism behind improvements made to electrochemical and thermal properties related to the concentration of residual lithium on the surfaces of Ni-rich compounds has not been reported as yet.

In this study, we synthesized Ni-rich $\text{LiNi}_{0.8}\text{Co}_{0.1}\text{Mn}_{0.1}\text{O}_2$ cathode materials with high discharge capacities and modified the surfaces by adding an amorphous carbon layer. To accomplish this, sugar was pyrolyzed to form a carbon layer on the active material. The aim of this work was to elucidate the relationship be-

*To whom correspondence should be addressed: Email: jt1234@ut.ac.kr

tween the transformation of residual lithium hydroxide by pyrolysis of sugar and the electrochemical/thermal properties. X-ray diffraction (XRD) analysis, scanning electron microscopy (SEM), transmission electron microscopy (TEM), differential scanning calorimetry(DSC), and electrochemical tests were performed to assess the effects of this new approach.

2. EXPERIMENTAL

2.1. Synthesis of $\text{LiNi}_{0.8}\text{Co}_{0.1}\text{Mn}_{0.1}\text{O}_2$

The $[\text{Ni}_{0.8}\text{Co}_{0.1}\text{Mn}_{0.1}](\text{OH})_2$ precursor was synthesized via co-precipitation. A 1 M aqueous solution of $\text{NiSO}_4 \cdot 6\text{H}_2\text{O}$, $\text{CoSO}_4 \cdot 7\text{H}_2\text{O}$, and $\text{MnSO}_4 \cdot 2\text{H}_2\text{O}$ was pumped into a 4 L tank reactor that was continuously stirred under N_2 atmosphere. At the same time, NaOH (2 M) and NH_4OH solutions were separately fed into the reactor. During the co-precipitation reaction, the newly formed particles grew into spherical particles under vigorous stirring. The resulting $[\text{Ni}_{0.8}\text{Co}_{0.1}\text{Mn}_{0.1}](\text{OH})_2$ particles were then filtered, washed, and dried in vacuum. The precursors and $\text{LiOH} \cdot \text{H}_2\text{O}$ were mixed at room temperature for 1 h. The mixed powder was calcined at 800 °C for 24 h in air and then slowly cooled to room temperature at a rate of 1 °C/min.

2.2. Carbon coating

Sugar powder ($\text{C}_{12}\text{H}_{22}\text{O}_{11}$, Aldrich) was dispersed in N-methyl pyrrolidone (NMP). Then, the $\text{LiNi}_{0.8}\text{Co}_{0.1}\text{Mn}_{0.1}\text{O}_2$ powders were slowly poured into the sugar solution. The starting ration of active material versus $\text{C}_{12}\text{H}_{22}\text{O}_{11}$ was 95:5 by weight. Then, the mixture was stirred at 60 °C for 4 h to induce the surface coating of the NCM powder particles. The mixed solution was filtered and then calcined at 700 °C for 12 h in air to obtain the carbon-coated $\text{LiNi}_{0.8}\text{Co}_{0.1}\text{Mn}_{0.1}\text{O}_2$ powders.

2.3. Material characterization

XRD using monochromatic $\text{Cu K}\alpha$ radiation ($\lambda = 1.5406\text{\AA}$) with an X-ray diffractometer in the 2θ range of 10 to 70° was used to identify the crystalline phase of the prepared powders. The samples were subjected to SEM (QUANTA 300, JEOL) before and after coating. The elemental distribution on the surfaces of the carbon-coated $\text{LiNi}_{0.8}\text{Co}_{0.1}\text{Mn}_{0.1}\text{O}_2$ particles was examined using energy dispersive spectroscopy (EDX). The surface morphologies of the powders were observed using field emission transmission electron microscopy (FETEM). DSC was used to determine the thermal stability of the cathode material. The analysis was undertaken with a DSC Q1000 (TA Co.) instrument. The sample was made by charging the coin cell to 4.3 V and then drying it for 24 h at 80 °C. The temperature range for the measurement was between 50 and 300 °C using a heating rate of 10 °C min⁻¹.

2.5. Electrochemical test

The electrochemical performance of the carbon-coated $\text{LiNi}_{0.8}\text{Co}_{0.1}\text{Mn}_{0.1}\text{O}_2$ powders was measured using a CR2032 coin-type cell. The cathode was fabricated by blending the active material, super-P carbon, and a binder (8:1:1) in N-methyl-2-pyrrolidone. The mixed slurry was cast uniformly onto a thin aluminum foil substrate and dried in a vacuum for 12 h at 120 °C. Lithium metal foil was used as the anode, a polypropylene microporous film was used as the separator, and the electrolyte consisted of 1 M LiPF_6 in a 3:7 (v/v) mixture of ethylene carbonate (EC) diethyl carbonate

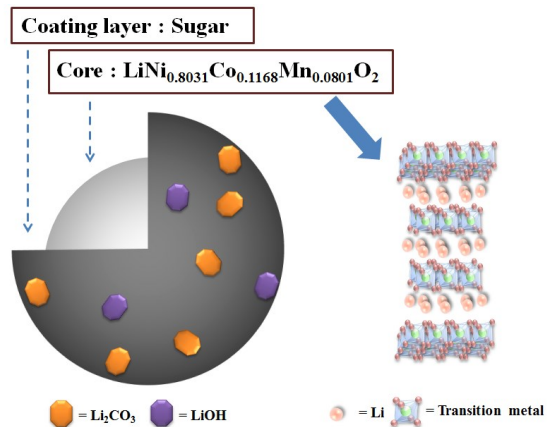


Figure 1. Schematic illustration of surface chemistry of $\text{LiNi}_{0.8}\text{Co}_{0.1}\text{Mn}_{0.1}\text{O}_2$ by pyrolysis of sugar.

(DEC). Finally, the cells were assembled in an argon-filled glove box. Electrochemical tests were performed between 3.0 and 4.3 V. AC impedance measurements of the cells were performed at a state of charge (SOC) of 0% using a Solatron 1287 electrochemical interface over the frequency range from 1 Hz to 155 Hz with an amplitude of 10 μA .

3. RESULTS AND DISCUSSION

3.1. Surface modification of $\text{LiNi}_{0.8}\text{Co}_{0.1}\text{Mn}_{0.1}\text{O}_2$

The chemical composition of the product was determined to be $\text{Li}_{0.98}\text{Ni}_{0.81}\text{Co}_{0.11}\text{Mn}_{0.10}\text{O}_2$ by inductively coupled plasma (ICP). Here, a small amount of deficient Li was thought to have been vaporized during calcining at 800 °C for 24 h.

The surface states of the carbon-coated $\text{LiNi}_{0.8}\text{Co}_{0.1}\text{Mn}_{0.1}\text{O}_2$ are illustrated in Fig. 1. Through LiOH and Li_2CO_3 titration, it was confirmed that the sugar successfully converted LiOH to Li_2CO_3 by pyrolysis as follows. The titration results are shown in Table 1. Because of the reduced content of LiOH , the coated material exhibited a lower pH value than did the uncoated material.



The surfaces of the uncoated powders were covered with a sig-

Table 1. pH value and titration results of residual lithium for uncoated and carbon-coated $\text{LiNi}_{0.8}\text{Co}_{0.1}\text{Mn}_{0.1}\text{O}_2$.

	Uncoated $\text{LiNi}_{0.8}\text{Co}_{0.1}\text{Mn}_{0.1}\text{O}_2$	Carbon-coated $\text{LiNi}_{0.8}\text{Co}_{0.1}\text{Mn}_{0.1}\text{O}_2$
LiOH (ppm)	3,782	2,156
Li ($\text{mol} \times 10^{-6}$)	157	90
Li_2CO_3 (ppm)	3,801	7,148
Li ($\text{mol} \times 10^{-6}$)	102	193
pH	11.3	10.5

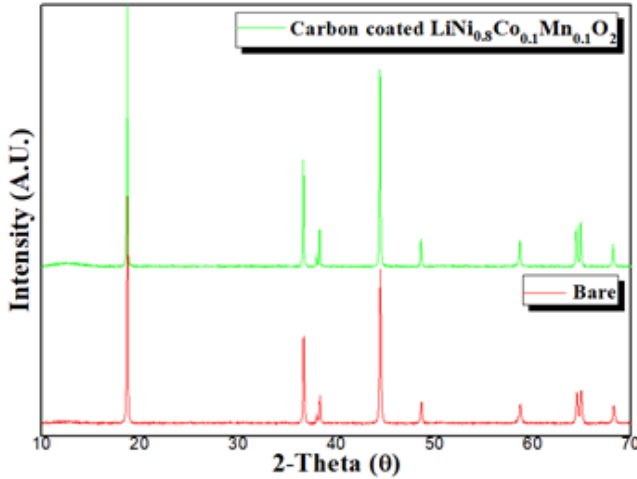


Figure 2. XRD patterns of the uncoated and carbon-coated $\text{LiNi}_{0.8}\text{Co}_{0.1}\text{Mn}_{0.1}\text{O}_2$.

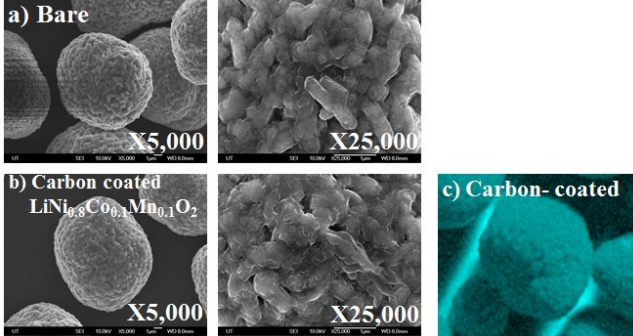


Figure 3. SEM images of (a) uncoated and (b) carbon-coated $\text{LiNi}_{0.8}\text{Co}_{0.1}\text{Mn}_{0.1}\text{O}_2$ particles and (c) EDS mapping images of carbon in the carbon-coated $\text{LiNi}_{0.8}\text{Co}_{0.1}\text{Mn}_{0.1}\text{O}_2$ particles.

nificant amount of residual lithium compounds that may cause significant resistance owing to the insulating characteristics of the compounds [18]. But, as we know, no reports have been published regarding the role of LiOH and Li_2CO_3 individually. Therefore, we report for the first time the results of the conversion of LiOH to Li_2CO_3 , which may change the electrochemical and thermal properties.

Fig. 2 shows the XRD patterns of the uncoated and carbon-coated $\text{LiNi}_{0.8}\text{Co}_{0.1}\text{Mn}_{0.1}\text{O}_2$ powders. The XRD patterns of all materials could be indexed on the basis of the $\alpha\text{-NaFeO}_2$ structure (space group: $R\text{-}3m$), and distinct splitting of the (006)/(012) and (018)/(110) peaks indicates that these oxides possessed a well-developed layered structure. This result indicates that the carbon process did not destroy the original layer structure of $\text{LiNi}_{0.8}\text{Co}_{0.1}\text{Mn}_{0.1}\text{O}_2$ [19]. The SEM images of the uncoated $\text{LiNi}_{0.8}\text{Co}_{0.1}\text{Mn}_{0.1}\text{O}_2$ and carbon-coated $\text{LiNi}_{0.8}\text{Co}_{0.1}\text{Mn}_{0.1}\text{O}_2$ are shown in Fig. 3. All particles had the form of spherical secondary particles constituting the primary particles of agglomerate-like. In comparing the uncoated to the coated $\text{LiNi}_{0.8}\text{Co}_{0.1}\text{Mn}_{0.1}\text{O}_2$ particles,

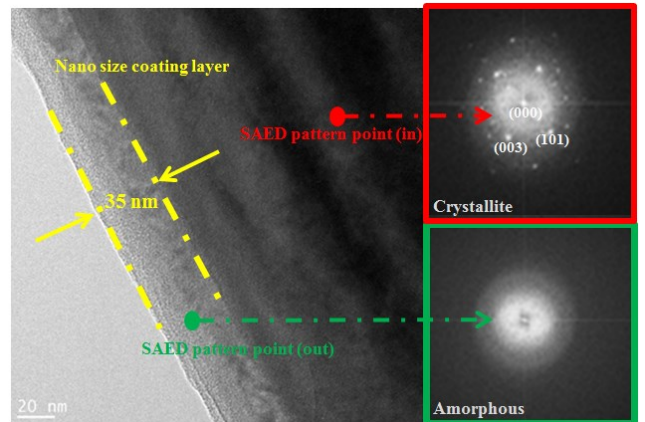


Figure 4. TEM image of carbon-coated $\text{LiNi}_{0.8}\text{Co}_{0.1}\text{Mn}_{0.1}\text{O}_2$ particle with SAED patterns

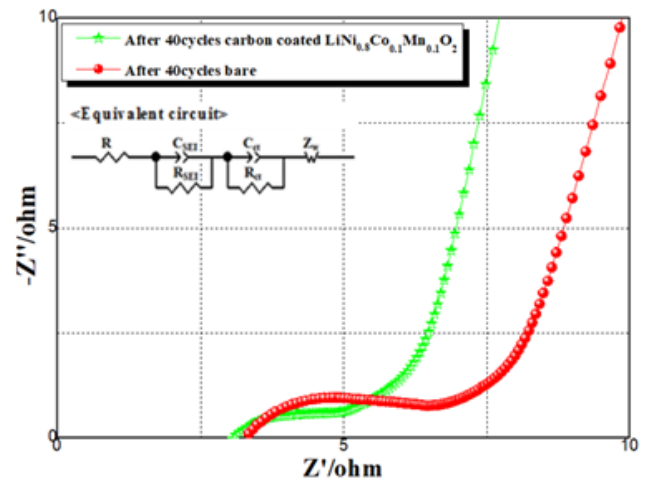


Figure 5. Nyquist plots of uncoated and carbon-coated $\text{LiNi}_{0.8}\text{Co}_{0.1}\text{Mn}_{0.1}\text{O}_2$ after 40th cycle.

we could not confirm the change in morphology as a result of the carbon coating. In order to confirm the carbon coating, the distribution of carbon on the particle surfaces was examined by EDS mapping and the results are shown in Fig. 3(c). The figure shows the uniform distribution of carbon arising from the pyrolysis of the sugar. In order to confirm the presence of the coating layer, Fig. 4 shows the TEM image of the carbon-coated $\text{LiNi}_{0.8}\text{Co}_{0.1}\text{Mn}_{0.1}\text{O}_2$. The edge of the carbon-coated $\text{LiNi}_{0.8}\text{Co}_{0.1}\text{Mn}_{0.1}\text{O}_2$ particle is covered with a thin layer (average thickness = 35 nm) of uniformly dispersed carbon. The selected area electron diffraction (SAED) pattern obtained from the carbon layer, outlined in Fig. 4 in green, exhibits a hollow ring pattern without bright spots, indicating that the coating layer consisted of an amorphous phase. The image outlined in red, taken from the $\text{LiNi}_{0.8}\text{Co}_{0.1}\text{Mn}_{0.1}\text{O}_2$ cathode material, shows some bright spots, which is typical for a crystalline $\text{LiNi}_{0.8}\text{Co}_{0.1}\text{Mn}_{0.1}\text{O}_2$ cathode material. Thus, these results provide conclusive evidence that the primary $\text{LiNi}_{0.8}\text{Co}_{0.1}\text{Mn}_{0.1}\text{O}_2$ particles are uniformly coated by a nano-sized amorphous carbon layer.

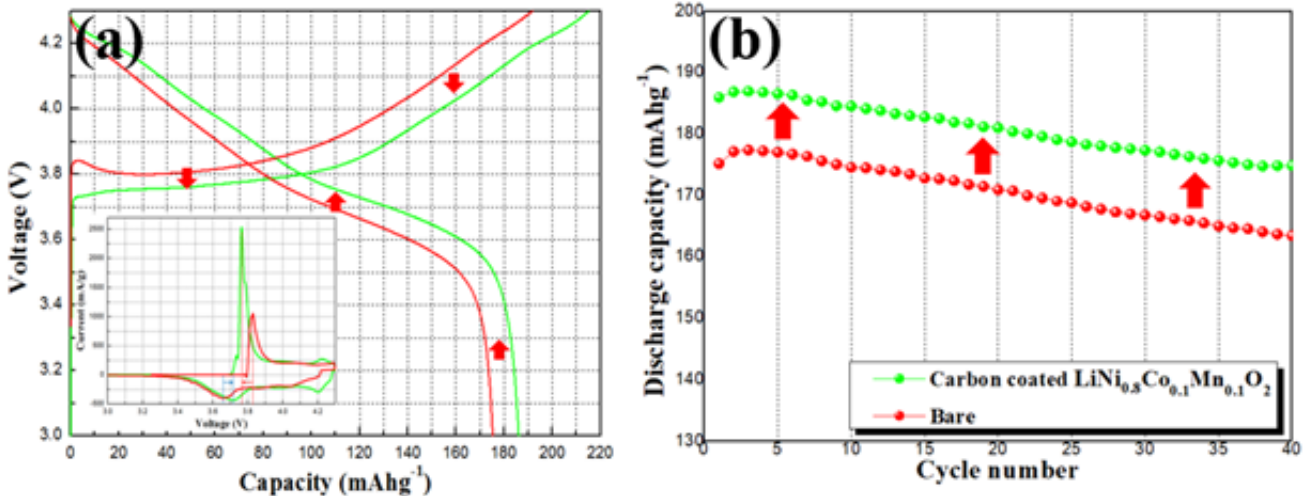


Figure 6. (a) Initial charge and discharge curves and (b) cycle performance of uncoated and carbon-coated $\text{LiNi}_{0.8}\text{Co}_{0.1}\text{Mn}_{0.1}\text{O}_2$ electrodes at a current density of 17 mA/g in a voltage range from 3.0 to 4.3 V.

3.2. Electrochemical impedance spectroscopy (EIS) test

Electrochemical impedance spectroscopy (EIS) can be used to investigate the kinetic process of lithium intercalation/deintercalation into electrodes. Fig. 5 shows the Nyquist plots of the uncoated and carbon-coated $\text{LiNi}_{0.8}\text{Co}_{0.1}\text{Mn}_{0.1}\text{O}_2$ electrodes during the 40th cycle in the charge state of 4.3 V. The high-frequency semicircle is attributed to the resistance of the solid electrolyte interphase (SEI) film (R_{SEI}), and the second semicircle appearing at a lower frequency is associated with the charge transfer resistance (R_{ct}). The carbon-coated $\text{LiNi}_{0.8}\text{Co}_{0.1}\text{Mn}_{0.1}\text{O}_2$ electrodes show an R_{ct} value of 4.7 Ω . On the other hand, the R_{ct} value for the uncoated NCS electrode increased significantly to 6.5 Ω . These results indicate that the carbon-coated $\text{LiNi}_{0.8}\text{Co}_{0.1}\text{Mn}_{0.1}\text{O}_2$ electrodes can improve the electrochemical properties of cathode materials.

3.3. Electrochemical test

Fig. 6(a) shows the initial charge/discharge curves for the uncoated and carbon-coated $\text{LiNi}_{0.8}\text{Co}_{0.1}\text{Mn}_{0.1}\text{O}_2$ electrodes at a current density of 17 mA/g (0.1 C) from 3.0 to 4.3 V. The initial charge and discharge capacities of the uncoated $\text{LiNi}_{0.8}\text{Co}_{0.1}\text{Mn}_{0.1}\text{O}_2$ electrodes were 191 mAhg^{-1} and 175 mAhg^{-1} , respectively. In contrast, the carbon-coated $\text{LiNi}_{0.8}\text{Co}_{0.1}\text{Mn}_{0.1}\text{O}_2$ electrodes exhibited initial charge and discharge capacities of 215 mAhg^{-1} and 186 mAhg^{-1} , respectively. Also, the carbon-coated $\text{LiNi}_{0.8}\text{Co}_{0.1}\text{Mn}_{0.1}\text{O}_2$ electrodes showed a slightly improved coulombic efficiency as compared to the uncoated electrode. Fig. 6(b) shows the cycle performance of the uncoated and carbon-coated $\text{LiNi}_{0.8}\text{Co}_{0.1}\text{Mn}_{0.1}\text{O}_2$ electrode at a current density of 17 mA/g (0.1 C) from 3.0 to 4.3 V. The initial discharge capacity of the uncoated $\text{LiNi}_{0.8}\text{Co}_{0.1}\text{Mn}_{0.1}\text{O}_2$ electrode decreased from 175 mAhg^{-1} to 163 mAhg^{-1} by the 40th cycle (40th cycle efficiency = 93%). The carbon-coated $\text{LiNi}_{0.8}\text{Co}_{0.1}\text{Mn}_{0.1}\text{O}_2$ electrode delivered an initial discharge capacity of 186 mAhg^{-1} , which decreased to 175 mAhg^{-1} after the 40th cycle (40th cycle efficiency = 94%). The enhanced cycle effi-

cency was the result of the lower LiOH content and the HF attack.

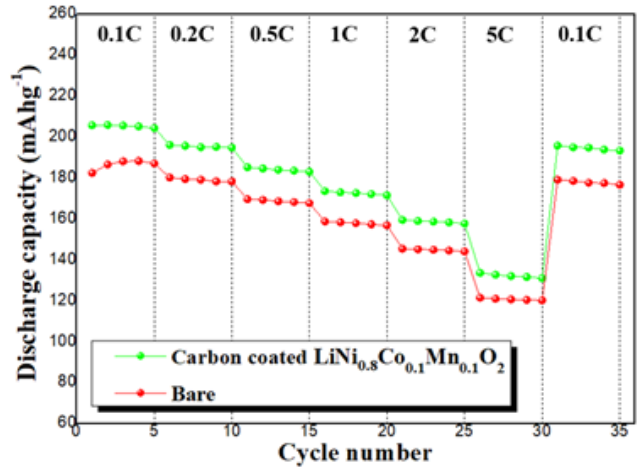


Figure 7. Rate capability curves for uncoated and carbon-coated $\text{LiNi}_{0.8}\text{Co}_{0.1}\text{Mn}_{0.1}\text{O}_2$ electrodes in the voltage range from 3.0 to 4.3 V at 0.1, 0.2, 0.5, 1, 2, and 5 0.1 C rate.

Because the SEI film is suppressed, R_{ct} is reduced, and so the insertion/extraction of Li^+ ions occurs more smoothly during the charge and discharge process. Fig. 7 shows the rate capability for the uncoated and carbon-coated $\text{LiNi}_{0.8}\text{Co}_{0.1}\text{Mn}_{0.1}\text{O}_2$ electrodes at various current densities. The carbon-coated $\text{LiNi}_{0.8}\text{Co}_{0.1}\text{Mn}_{0.1}\text{O}_2$ electrode exhibited a higher capacity efficiency than the uncoated $\text{LiNi}_{0.8}\text{Co}_{0.1}\text{Mn}_{0.1}\text{O}_2$ electrode for every rate, which further demonstrates the improvement in the rate capability. These results suggest that easier lithium intercalation/deintercalation is responsible for reducing the charge transfer resistance. Fig. 8 shows the DSC curves for the uncoated and carbon-coated $\text{LiNi}_{0.8}\text{Co}_{0.1}\text{Mn}_{0.1}\text{O}_2$ materials in a charged state at 4.3 V. The uncoated

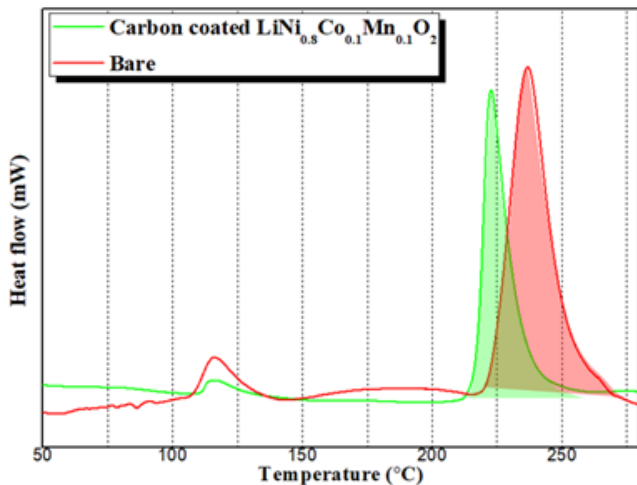


Figure 8. DSC curves for uncoated and carbon-coated $\text{LiNi}_{0.8}\text{Co}_{0.1}\text{Mn}_{0.1}\text{O}_2$ electrodes.

$\text{LiNi}_{0.8}\text{Co}_{0.1}\text{Mn}_{0.1}\text{O}_2$ material had a large exothermic peak at 236.73 °C and a released reaction heat of 458.6 J/g. In contrast, the carbon-coated $\text{LiNi}_{0.8}\text{Co}_{0.1}\text{Mn}_{0.1}\text{O}_2$ electrode material had a reaction at a higher temperature of 222.73 °C with a released heat of 345.8 J/g. These results clearly show that the carbon-coated $\text{LiNi}_{0.8}\text{Co}_{0.1}\text{Mn}_{0.1}\text{O}_2$ material had a lower released heat than the uncoated $\text{LiNi}_{0.8}\text{Co}_{0.1}\text{Mn}_{0.1}\text{O}_2$ material but fast release oxygen ions at lower temperature.

4. CONCLUSIONS

In this study, we modified the $\text{LiNi}_{0.8}\text{Co}_{0.1}\text{Mn}_{0.1}\text{O}_2$ surface with sugar ($\text{C}_{12}\text{H}_{22}\text{O}_{11}$), resulting in carbon-coated $\text{LiNi}_{0.8}\text{Co}_{0.1}\text{Mn}_{0.1}\text{O}_2$ through a reaction with residual LiOH compounds present on the surfaces of the $\text{LiNi}_{0.8}\text{Co}_{0.1}\text{Mn}_{0.1}\text{O}_2$ particles. The LiOH was converted to Li_2CO_3 during the pyrolysis reaction of sugar. This was effective and economical in reducing the concentration of residual LiOH on the surfaces of the $\text{LiNi}_{0.8}\text{Co}_{0.1}\text{Mn}_{0.1}\text{O}_2$ particles. As a result, the carbon-coated $\text{LiNi}_{0.8}\text{Co}_{0.1}\text{Mn}_{0.1}\text{O}_2$ exhibited better capacity retention, improved rate capabilities, and lower impedance growth than the uncoated $\text{LiNi}_{0.8}\text{Co}_{0.1}\text{Mn}_{0.1}\text{O}_2$. These improvements were mainly attributed to the presence of the carbon layers, which lowered the concentration of LiOH and protected the active material from HF attack during cycling. These multiple functions of the carbon coating layer had positive effects on the electrochemical performance and reduced the released heat during ignition.

The PE coating layer effectively inhibited the formation of the SEI film after a 4.3 V initial charge process. R_{SEI} decreased as a result of the reduction in the SEI film. In addition, the decrease in R_{SEI} improved the lithium intercalation/deintercalation and reduce R_{ct} . These results indicate that the reduction in the initial capacity of the non-active coating layer was not confirmed, and the efficiency improved to 94.6% at the 30th cycle. In particular, the DSC analysis revealed that the 0.wt% PE-coated NCS material possessed improved thermal stability through a reduction in the heat generated and an increase in the exothermic peak. This work is the first report on the conversion of LiOH to Li_2CO_3 , which may change the

electrochemical and thermal properties of $\text{LiNi}_{0.8}\text{Co}_{0.1}\text{Mn}_{0.1}\text{O}_2$.

5. ACKNOWLEDGMENTS

This study was supported by the granted financial resource from the Ministry of Trade program of the Industry & Energy, Republic of Korea (G02N03620000901) and Business for R&D funded Korea Small and Medium Business Administration in 2017 (C05098480100470152).

REFERENCES

- [1] M. Armand and J. M. Tarascon, Nature, 451, 652 (2008).
- [2] A. Kraysberg and Y. Ein-Eli, Adv. Energy. Mater., 2, 922 (2012).
- [3] J. M. Tarascon and M. Armand, Nature 414, 359 (2001).
- [4] H. L. Wang, Z. Q. Shi, J. W. Li, S. Yang, R. B. Ren, J. Y. Cui, J. L. Xiao, and B. Zhang, J. Power Sources, 288, 206 (2015).
- [5] Z. Zhu, H. Yan, D. Zhang, W. Li, and Q. Lu, J. Power Sources, 224, 13 (2013).
- [6] J. J. Wang and X. L. Sun, Energy. Environ. Sci., 8, 1110 (2015).
- [7] H. J. Noh, S. J. Youn, C. S. Yoon, and Y. K. Sun, J. Power Sources, 233, 121 (2013).
- [8] Q. Liu, K. Du, H. W. Guo, Z. D. Peng, Y. B. Cao, and G. R. Hu, Electrochimica Acta, 90, 350 (2013).
- [9] D. H. Cho, C. H. Jo, W. S. Cho, Y. J. Kim, H. Yashiro, Y. K. Sun, and S. T. Myung, J. Electrochem. Soc., 161, A920 (2014).
- [10] M. Bettge, Y. Li, B. Sankaran, N. D. Rago, T. Spila, T. T. Haasch, I. Petrov, and D. P. Abraham, J. Power Sources, 233, 346 (2013).
- [11] S. T. Myung, K. Izumi, S. Komaba, H. Yashiro, H. J. Bang, Y. K. Sun, and N. Kumagai, J. Phy. Chem. C., 111, 4061 (2007).
- [12] A. T. Appapillai, A. N. Mansour, J. P. Cho, and Y. Shao-Horn, Chem. Mater., 19, 5748 (2007).
- [13] Y. C. Lu, A. N. Mansour, N. Yabuuchi, and Y. Shao-Horn, Chem. Mater., 19, 4408 (2009).
- [14] H. Huang, S. C. Lin, and L. F. Nazar, Solid-State Lett., 4, A170 (2001).
- [15] B. L. Cushing and J. B. Goodenough, Solid State Sci., 4, 1487 (2002).
- [16] Q. Cao, H. P. Zhang, G. J. Wang, Q. Xia, Y. P. Wu, and H. Q. Wu, Electrochim. Commun., 9, 1228 (2007).
- [17] T. Hwang, J. K. Lee, J. Mun, and W. Choi, J. Power Sources, 322, 40 (2016).
- [18] D. Aurbach, M. D. Levi, E. Levi, B. Markovsky, G. Salitra, H. Teller, U. Heider, and L. Heider, Mater. Res. Soc. Symp. Proc., 496, 435 (1998).
- [19] B. Lin, Z. Wen, J. Han, and X. Wu, Solid State Ionic, 179, 1750 (2008).

